SLAC-PUB-2887
March 1982
(T/E)

CHARMONIUM SPECTROSCOPY FROM INCLUSIVE PHOTONS IN J/ψ AND ψ' DECAYS*

John E. Gaiser
(Representing the Crystal Ball Collaboration)[1]
Stanford Linear Accelerator Center
Stanford University, Stanford, California 94305

ABSTRACT

The Crystal Ball detector at SPEAR is used to study the inclusive photon spectra in decays of the J/ψ and ψ', with double our previous data sample. Branching fractions for $\psi' \to \gamma\chi_{0,1,2}$ have been measured as $(9.7 \pm 0.6)\%$, $(8.8 \pm 0.5)\%$ and $(7.7 \pm 0.5)\%$ respectively. Combining measurements from inclusive and exclusive Crystal Ball studies our best values for the natural widths are, $\Gamma_{tot}(\chi_{0,1,2}) = (16 \pm 4)$, <2.6 (90% C.L.), and (3 ± 2) MeV respectively; and the radiative widths $\Gamma(\chi_{0,1,2} \to \gamma J/\psi)$ are (97 ± 38), <700 (90% C.L.), and (490 ± 330) KeV respectively. By assuming naive E1 theory for $\chi_{0,1} \to \gamma J/\psi$, we obtain an estimate for $\Gamma_{tot}(\chi_1) = (0.75 \pm 0.50)$ MeV. Performing a simultaneous fit to the decays $\psi' \to \gamma\eta_c$ and $J/\psi \to \gamma\eta_c$ we measure the branching fractions as $(0.29 \pm 0.08)\%$ and $(1.20 +0.53,-0.35)\%$ respectively, for a mass of 2984 ± 5 MeV and a natural line width of 12.4 ± 4.6 MeV. An η_c' candidate state is observed with mass $M = 3592 \pm 5$ MeV, natural line width $\Gamma_{tot} < 8$ MeV (95% C.L.), and $BR(\psi' \to \gamma\eta_c'$ candidate$) = (0.2\text{-}1.3)\%$ (95% C.L.).

(Invited talk presented at the XVIIth Rencontre de Moriond: Workshop on New Flavours, Les Arcs, France, January 24-30, 1982.)

* Work supported by the Department of Energy, contract DE-AC03-76SF00515.

1. INTRODUCTION

Precise measurements of the heavy quarkonium spectroscopies is crucial to the current efforts at formulating a theory for strongly bound systems. In particular, charmonium below threshold, with its high production rates in e^+e^- ($\simeq$200K resonance events/week), allows for a detailed study of the radiative transitions and provides a basic test for the quarkonium models and QCD. We report here on inclusive photon spectra obtained using the Crystal Ball NaI(Tl) detector at SPEAR, comprising 1.8×10^6 ψ' and 2.2×10^6 J/ψ (±5% overall systematic), with an integrated luminosity of 3450 nb^{-1} and 765 nb^{-1} respectively.

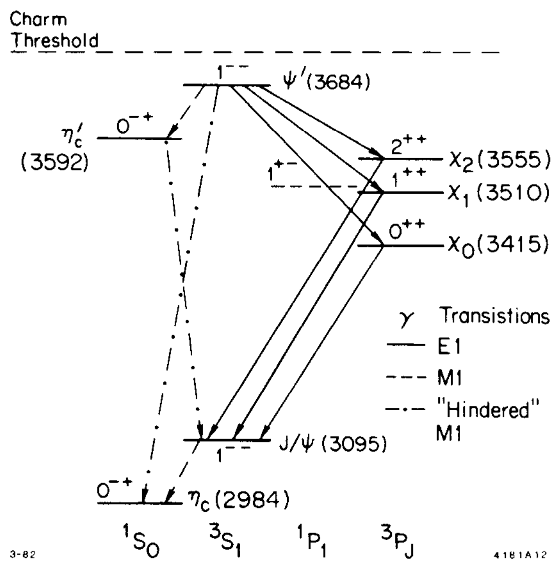

Fig. 1. Charmonium level scheme.

Figure 1 illustrates the charmonium scheme, indicating the quantum numbers J^{PC} with the spectroscopic notation $^{2s+1}L_J$. Not all of the possible radiative transitions are shown, but all those currently observed are present. Regarding the current experimental situation, aside from the well established triplet S and P wave states, the J/ψ hyperfine partner, $\eta_c(2984)$ is seen both in inclusive[2] and exclusive[2,3] channels but lacks measurement of its spin-parity quantum numbers; the recently observed ψ' hyperfine partner, $\eta_c'(3592)$ candidate,[4] is seen only inclusively; and the singlet $^1P_1$ state has never been seen[5] (having negative C-parity, its detection is expected to be difficult).

After the discoveries of J/ψ and ψ' (1974) three experiments measured the inclusive photon spectra with increasing degrees of sensitivity. The first attempt by a two crystal NaI(Tl) detector,[6] could only place upper limits on radiative transitions because of low statistics and a low photon efficiency. A magnetic detector[7] measuring converted photons observed the $\psi' \to \gamma\chi_0$ transition, but was insensitive to photons below 200 MeV. A moderately segmented NaI(Tl) detector[8] with data from a short run at SPEAR measured the transitions to each of the triplet P states and observed the secondary γ transitions to J/ψ.

2. DETECTOR AND ANALYSIS

The Crystal Ball detector consists of a highly segmented array of NaI(Tl) crystals (98% of 4π steradians) for high-resolution measurements of the photon energy, position (1^o-2^o resolution depending on energy), and lateral energy distributions; centrally located spark and proportional chambers are used for charged particle recognition. A more complete description may be found in the references.[9,10]

Detailed aspects of the analysis, i.e., the event selection, the photon selection, the fits to the inclusive photon spectra, and the estimations of the photon efficiency, have been described elsewhere.[11] We will present a summary here. Hadronic events were software selected (efficiency 94%) from the trigger sample which also contained the following backgrounds: cosmic rays, beam-gas interactions, QED, and direct resonance decays to a lepton pair. The dominant residual contamination (from the first two items) is 0.5% at J/ψ and 1.2% at ψ'. The nonresonance physics background is 1.4% at J/ψ and 4.3% at ψ'. The trigger efficiency for hadronic decays is >98%.

Of central importance in our spectroscopic studies was the detailed examination of the radiative transitions involving the χ_J states to test for systematic errors resulting from the background shape under the peaks, and the estimations of the photon efficiencies. Widely different selection criteria for defining neutral tracks were employed, leading to sets of spectra for J/ψ and ψ'. The degree of selection (in order of increasing enhancement of signal to background) ranged from a spectrum of all tracks (neutral and charged), Fig. 2(a), to a highly restricted spectrum, Fig. 2(b), based on the following cuts: i) removal of charged particles after identification by the central chambers [efficiency $\simeq$(85-90)%]; ii) neutral tracks overlapping interacting hadronic showers were removed; iii) photons which could be reconstructed to a π^0 mass were cut; and iv) residual charged particles (missed by the tracking chambers) were identified by their lateral energy distribution in the adjacent crystals and cut.

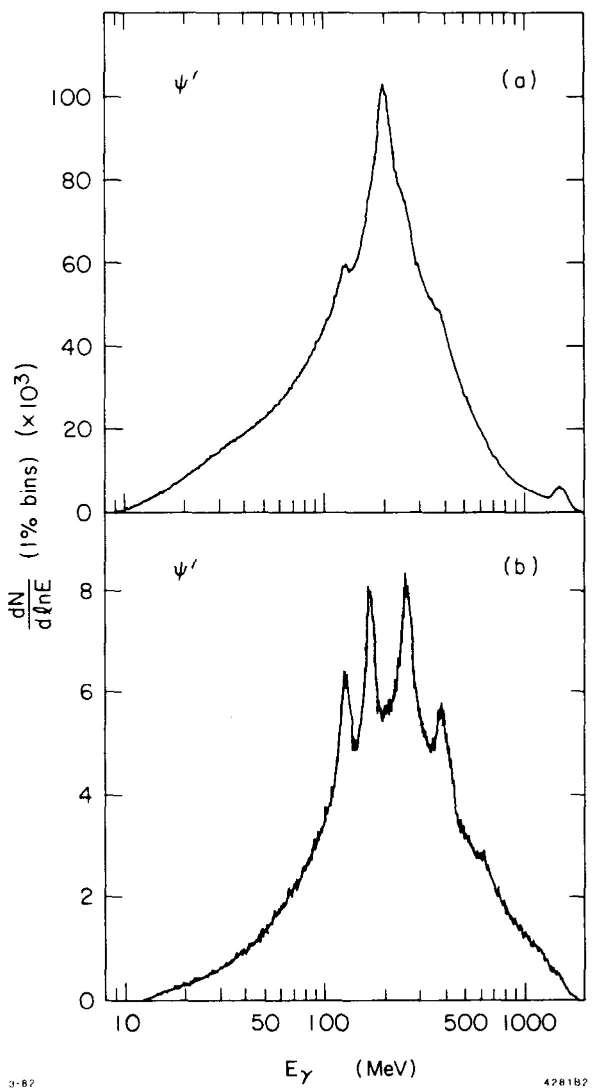

Fig. 2. Inclusive γ spectra at ψ'.

The signals in the resulting spectra were fit with the known detector NaI(Tl) line shape and resolution, and in the event of a broad state, folded with a nonrelativistic Breit-Wigner mass distribution. In fitting the backgrounds, terms were included for the following: i) an amplitude for our measured charged particle spectrum; ii) an amplitude for the Monte Carlo generated spectrum $\psi' \to \pi^0\pi^0 J/\psi$ for the ψ' spectra without π^0 subtraction, and an amplitude for a similarily generated spectrum $\psi' \to \eta J/\psi$ for all ψ' spectra, and iii) a sum of Legendre polynomials of order 2 to 5 (depending on the size of the energy interval in the fit), for the remaining broad photon background. Figures 3(a) and (b) show fits to the ψ' spectra in Figs. 2(a) and (b) respectively, for the χ_J transitions.

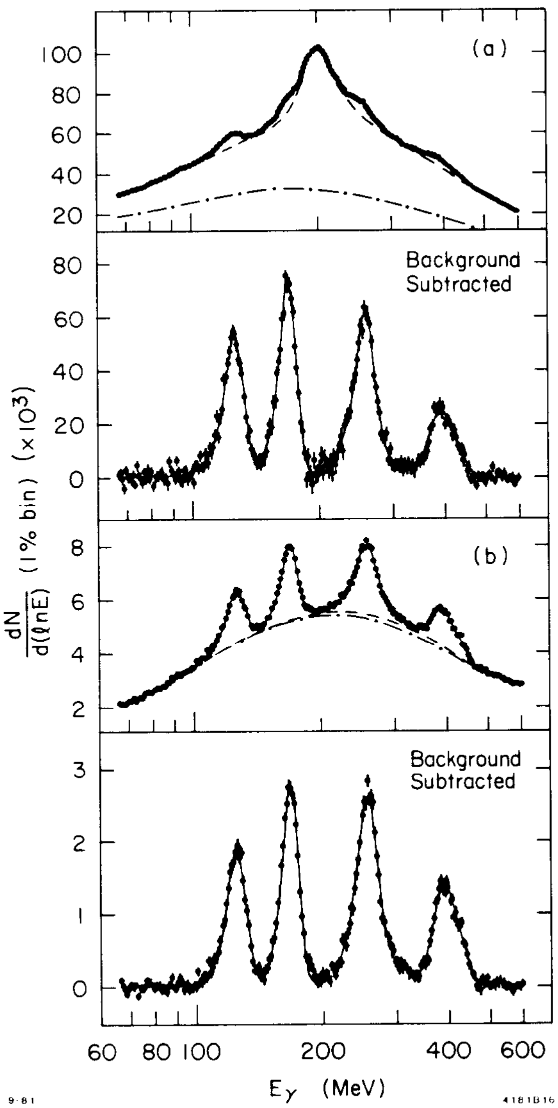

Fig. 3. Fits to χ_J transitions at ψ'.

Estimates of the photon detection efficiencies, using a Monte Carlo, were made at 5 photon energies spanning the observed χ peaks, for each spectrum in the study. Monochromatic photons were generated isotropically, propogated through the Crystal Ball Monte Carlo using the EGS electromagnetic shower code,[12] added to real J/ψ events, analyzed with the production programs, and combined with the ψ' spectra. The photon efficiencies for these ψ' events were obtained from the fitted Monte Carlo signal strengths. A similar procedure was carried out for the J/ψ spectra yielding efficiencies identical with the ψ' results within statistical errors. Additional corrections were made for the photon conversion probability and the measured recoil γ angular distributions ($1+\cos^2\theta$ for the η_c, η_c', and χ_0, $1-0.189\cos^2\theta$ for the χ_1, and $1-0.052\cos^2\theta$ for the χ_2).[10,13]

Consistent results were obtained for the BR($\psi' \to \gamma\chi_J$) and the χ_J natural width among the four different spectra in the study for each χ_J. Firstly this gives confidence to the quality of the estimations for the photon detection efficiency. Secondly, since the most distinguishing feature separating the three χ_J peaks is the variation in the underlying background, the observed consistency between spectra of considerably different backgrounds gives confidence to the accuracy of the point to point measurements within a given spectrum. Finally, the inclusive results obtained for the product BR($\psi' \to \gamma\chi_J \to \gamma\gamma\psi$) are consistent with Crystal Ball exclusive measurements,[10] adding validity to the absolute values.

A similar study (with five spectra) was carried out for the transitions $\psi' \to \gamma\eta_c$ and $\psi \to \gamma\eta_c$, where the ψ' and J/ψ spectra were fit simultaneously to the same mass $[M(\eta_c)]$ recoiling against the photons. Examples of the J/ψ and ψ' sepctra used in the η_c study are shown in Figs. 4(a) and (b); the corresponding simultaneous fit is shown in Figs. 5(a) and (b). Again the branching ratio and η_c natural width were found to be consistent among the selected spectra. With the confidence gained through these studies a particular photon selection criterion was chosen for examining the transition $\psi' \to \gamma\eta_c'$ (candidate). Figure 6 shows the resulting ψ' spectrum and fit used in the measurement of the $\psi' \to \gamma\eta_c'$ transition.

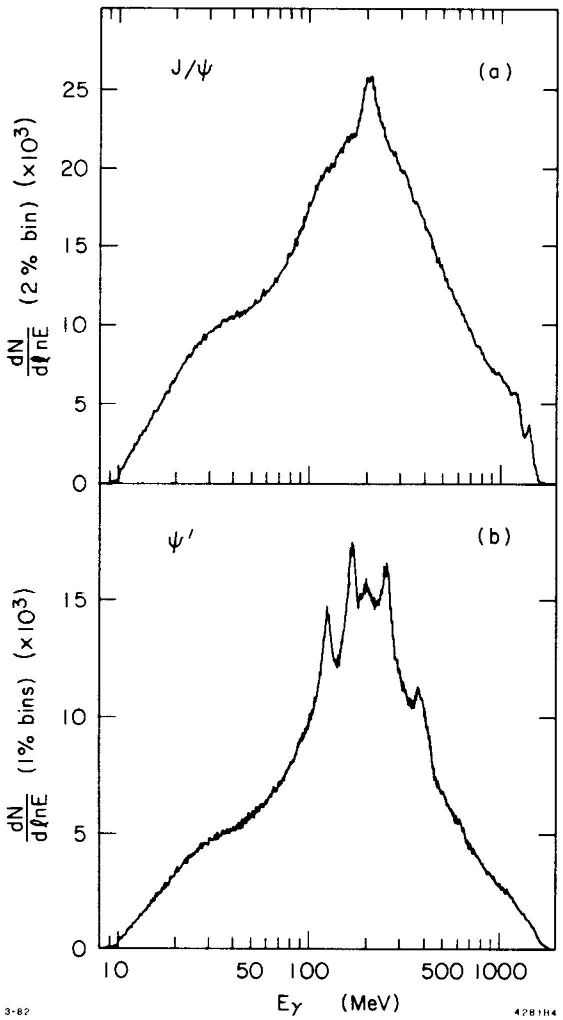

Fig. 4. Inclusive γ spectra at J/ψ and ψ' used for η_c study.

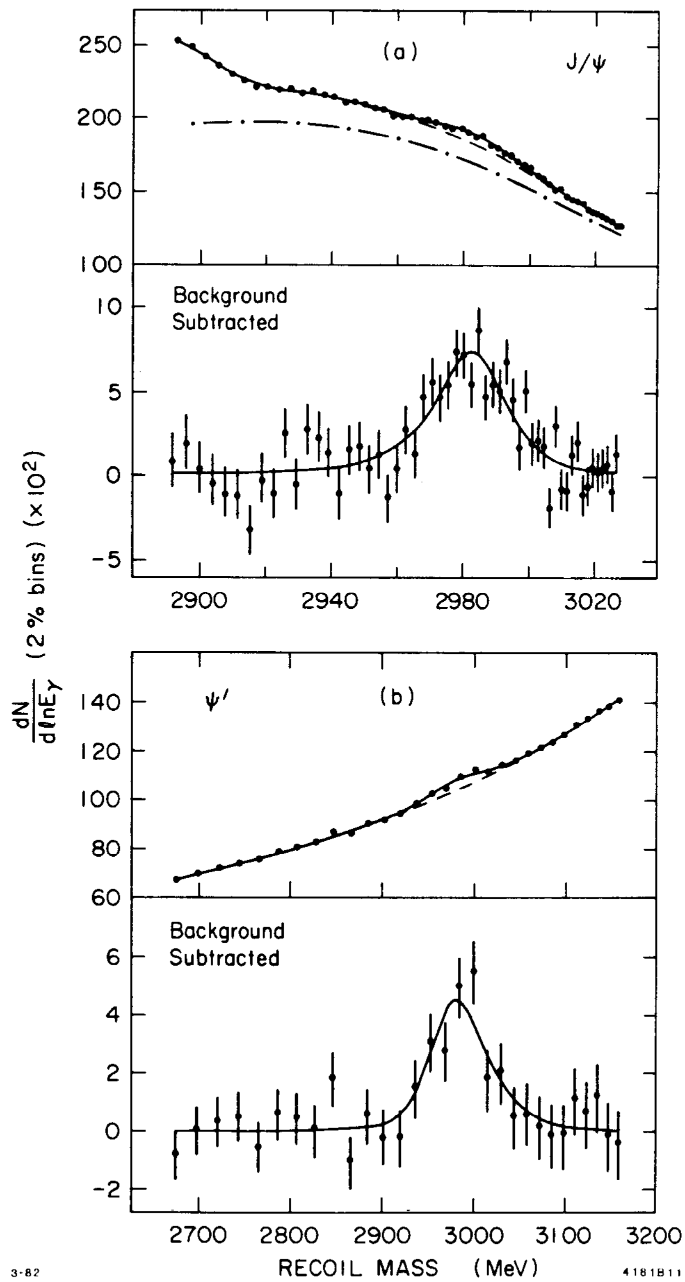

Fig. 5. Fits to η_c transitions.

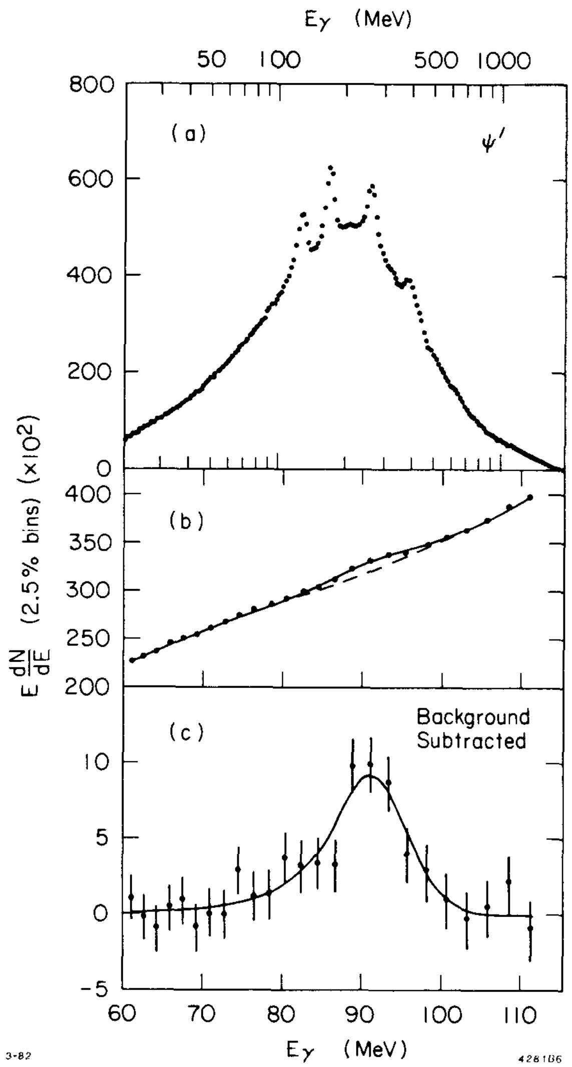

Fig. 6. Inclusive γ spectrum at ψ' and fit for η_c' study.

3. CHARMONIUM MODELS

Since as yet no field theory of the strong interactions has been able to explicitly solve the heavy quark-antiquark bound system problem, a major effort has been directed towards the employment of an instantaneous potential in conjunction with the experience gained from QED as a vehicle to carry out the desired calculations. The simplest model assumes a nonrelativistic system with a spin independent central potential. The spectrum and wave functions are obtained by solving the Schrödinger equation. Since QCD suggests only the asymptotic form of the potential (short distance and long distance) a variety of functions (and derivations) for the intermediate region have been tried.[14-19] The approach may be modified by including effects due to coupling with nearby states above and below the charm threshold.[15] Spin and relativistic effects may be calculated perturbatively.[20] Uncorrected limits on the E1 rates can also be estimated by using dipole sum rules.[21]

More complex approaches include spin dependence via a Breit-Fermi Hamiltonian borrowed from QED.[22,23] Assumptions regarding the Lorentz structure of the potential and the relative strengths of the different terms (spin-orbit, spin-spin, and tensor) must be made. There is the added possibility of a long range spin dependence which does not exist in QED. Recently the analog of the Breit-Fermi equation has been calculated from QCD for an arbitrary potential, without the necessity of inputting a Lorentz structure.[24] The Klein-Gordon equation was used in another approach, with a static potential to gauge the effect of relativistic wave functions on the E1 rates.[25] In addition relativistic corrections can be applied consistently to the electric dipole rate formula.[26] Relativistic sum rules have provided a corrected estimate of the relative E1 rates.[27] It is possible to avoid the nonrelativistic assumption and retain the use of an instantaneous potential with spin dependence and a particular Lorentz structure by solving the Salpeter integral equation of motion.[28] In this case relativistic wave functions are also obtained. Others have calculated the leading QCD corrections.[29,30]

An approach independent of potential models, based on the calculable aspects of QCD, such as gluonic vacuum expectation values, perturbative amplitudes, and dispersion relations,[31-33] attempts a "first principles" formulation (sum rules are derived). The procedure includes relativistic effects, the non-Abelian and noninstantaneous nature of the gluonic field, and couplings to mixed states. Although the methods are formalized and not ambiguous, they do not lend themselves to generalizations, which means a rather lengthy calculation for each prediction.

We make comparisons between our results and those theories listed in Table I which typify the various approaches to understanding the charmonium system. To assist the reader in the discussion and tables that follow, we assign each model a mnemonic.

4. RESULTS

4.1. $\psi' \to \gamma\chi_J$

Table II[34] summarizes the results obtained from the inclusive photon measurement for the E1 transitions $\psi' \to \gamma\chi_J$. The branching ratios from the earlier SPEAR experiment[8] are within the errors and slightly lower than our values. The next six nonrelativistic potential model predictions are generally consistent with each other, roughly a factor of two larger than measured, and within the upper bound of the nonrelativistic sum rule prediction (NONREL SR). The first order E1 rate formula used in these predictions is

$$\Gamma(\psi' \to \gamma\chi_J) = (4/27)(2J+1)Q^2\alpha|\langle\psi_f|r|\psi_i\rangle|^2 K_\gamma^3 \qquad (1)$$

where Q is the quark charge, α is the QED fine structure constant, ψ_f and ψ_i are the final and initial wave functions respectively, and K_γ is the photon energy from experiment. There are no corrections for i) higher multipoles, from interference of the photon wave function with the bound state ($e^{ikx} \neq 1$), or ii) relativistic effects. Since each model contributes only through the transition dipole matrix element, it might be concluded that collectively the wave functions are $\simeq\sqrt{2}$ too large. Rather it has been observed that the degree of coincidence of the P wave function peak with the 2S wave function node can significantly reduce the size of the matrix element.[22] From the Schrodinger equation the nonrelativistic potential models, which are similar in the 0.1 to 1.0 fermi region, derive similar center of gravity P wave functions. They do not reflect possible attractive and repulsive forces due to spin and relativistic effects, which can decrease the amount of overlap. Likewise, the relative rates in these models reduce to the naive E1 theory ratio 1:1:1, also in disagreement with measurement.

TABLE I. List of models used for comparison with data.

DESCRIPTION OF MODELS	MNEMONIC
<u>Nonrelativistic Potential, No Spin Dependence</u>	
Linear + Coulomb, fit to $M_{\psi'}$, M_{ψ}, $M_{^3P_J}$ c.o.g.[15] or Γ_{ee};[14] from asymptotic QCD.	NONREL L+C
Logarithmic, fit to $M_{\psi'}$, M_{ψ}; from $M_{\psi'} - M_{\psi} \cong M_{T'} - M_{T}$.[16]	NONREL LOG
QCD inspired, no free parameters; from QCD asymptotic q^2 dependence.[17]	NONREL QCD
Inverse scattering algorithm, fit to $c\bar{c}$ known spectrum, Γ_{ee}; from theory for one dimensional potentials.[18]	NONREL IS
Coupled channel model with linear + Coulomb, fit to $M_{\psi'}$, M_{ψ}, and Γ_{ee}; mixes $c\bar{c}$ states; modifies wave functions.[15]	NONREL CC
Thomas-Reiche-Kuhn and Wigner-Kirkwood sum rules.[21]	NONREL SR
<u>Relativistic/Spin Dependent</u>	
Salpeter equation, Coulomb (vector) + linear (scalar), relativistic kinematics to all orders in v/c, spin dependence, mixing, relativistic wave functions, variable α_s given by asymptotic freedom; fit to M_{ψ}, $M_{\psi'}$, $M_{^3P_J}$, $J = 0,1,2$.[28]	SAPLETER
Breit-Fermi Hamiltonian with Coulomb (vector) + linear (scalar) potential, all $(v/c)^2$ corrections included; fit to M_{ψ}, M_{χ_J}; from instantaneous approximation to Bethe-Salpeter equation.[22]	BF L+C
BAG model analog of Breit-Fermi Hamiltonian with all $(v/c)^2$ corrections; fit to M_{ψ}, M_{η_c}, $M_{\psi'}$; from adiabatic fixed BAG model (we use their fit A).[23]	BAG
Klein-Gordon equation with static Coulomb + linear (scalar) potential, gets corrections to naive E1 rates due to use of relativistic wave function.[25]	KG
E1 rates formula corrected to $(v/c)^2$, uses Breit-Fermi Hamiltonian with Coulomb + S.H.O. for confining.[26]	REL E1
Perturbative calculation of spin + relativistic effects starting with naive linear + Coulomb model; fit to M_{ψ}, $M_{\psi'}$, $M_{\psi''}$, M_{χ_0}, M_{χ_1}.[20]	PERT
Drell-Hearn relativistic sum rules.[27]	REL SR
<u>QCD Field Theoretic</u>	
Spin dependent potential from QCD, with relativistic corrections (Eichten-Feinberg equation), fit to M_{ψ}, $M_{\psi'}$, M_{χ} c.o.g.[24]	REL QCD
QCD field theory calculation, includes quark-gluon duality, spin + relativistic effects, and mixing. Calculable QCD quantities are related to physical quantities via dispersion theory and derived sum rules.[31-33]	DISP + SR
<u>QCD Corrections</u>	
QCD radiative corrections to HFS, and widths.[29]	QCD RADCOR
One gluon QCD corrections to E1 theory.[30]	QCD E1

TABLE II. ψ' E1 transitions.

DATUM	χ_0	χ_1	χ_2
BR($\psi' \to \gamma\chi_J$)			
Crystal Ball[a]	0.097 ± .006 ± .016	0.088 ± .005 ± .014	0.077 ± .005 ± .012
SP-27[8]	0.072 ± .023	0.071 ± .019	0.070 ± .020
NONREL L+C[15]	0.23 ± .04	0.21 ± .04	0.13 ± .03
NONREL L+C[14]	0.20 ± .04	0.18 ± .03	0.13 ± .02
NONREL LOG	0.27 ± .05	0.23 ± .04	0.17 ± .03
NONREL QCD	0.27 ± .05	0.23 ± .04	0.18 ± .03
NONREL IS	0.24 ± .05	0.21 ± .04	0.16 ± .03
NONREL CC	0.20 ± .04	0.16 ± .03	0.11 ± .02
NONREL SR	< 0.30	< 0.26	< 0.19
SALPETER	0.10 ± .02	0.098 ± .018	0.065 ± .012
BF L+C	0.088 ± .016	0.13 ± .02	0.13 ± .02
BAG	0.11 ± .02	0.12 ± .02	0.11 ± .02
KG	0.18 ± .03	0.16 ± .03	0.12 ± .02
REL E1	0.085 ± .016	0.11 ± .02	0.089 ± .016
DISP + SR[32]	0.05 ± .01	--	--
DISP + SR[33]	0.035 ± .007	0.16 ± .04	0.15 ± .03
Relative Rates[c]			
Observed K_γ (MeV)[b]	258	170	126
Crystal Ball	1.00 ± .07	1.05 ± .08	1.37 ± .09
Naive E1 Theory	1	1	1
SALPETER	1	1.14	1.12
BF L+C	1	1.72	2.53
KG	1	1.04	1.14
REL E1	1	1.4	2.6
QCD E1	1	1.6 ± .1	1.90 ± .3
REL SR	1	1.3	1.2

a First error is point to point, second is overall normalization.
b The error in K_γ is dominated by a (1-2)% systematic error in calibration.
c Normalized by $1/(K_\gamma^3(2J+1))$.

The last 7 predictions in Table II include spin and relativistic dependence to various degrees. Aside from REL E1 and DISP + SR they rely on formula (1) and exhibit a common diminution in the rate solely from a smaller matrix element. REL E1 includes relativistic corrections to dipole formula (1), while DISP + SR, a dispersion calculation not using (1), also predicts lower rates. Since different wave functions for each χ_J are produced, reflecting variations in the spin coupling, the ratio of rates departs from the naive E1 theory equality, generally in the direction observed.

Space does not allow for a detailed examination of how well the models fit the charmonium mass spectrum and also the E1 rates. The latter appears to be a measure of how faithfully the actual wave functions are reproduced. In this regard the inclusion of spin and relativistic effects is a necessary aspect.

4.2. $\Gamma_{tot}(\chi_J)$

To obtain our best measurement for the χ state natural widths (Γ_{tot}) we combined the results from the inclusive process $\psi' \to \gamma\chi_J$ with results from the exclusive decay $\psi' \to \gamma\chi_J \to \gamma\gamma\psi \to \gamma\gamma\ell^+\ell^-$ (see Table III).[10] In both cases the first gamma's signal was fit with the detectors line shape and resolution folded with a nonrelativistic Breit-Wigner. One can write a formal relation for the extraction of Γ_{tot} as follows:

$$\Gamma_{tot} = f\Big(g(\mathrm{FWHM}) - h(\mathrm{RESOLUTION})\Big) \quad , \qquad (2)$$

where f, g and h correspond to a functional relation somewhere between quadratic and linear subtraction.[35] When Γ_{tot} is small compared to the resolution, both the resolution and the FWHM measurement require precission to obtain a significant measure of Γ_{tot}.

Considering the inclusive photon data first, the high statistics translates into values for the FWHM with a relative error in the FWHM $\simeq\pm0.2\%$, while the uncertainty in the resolution is $\simeq\pm7\%$. Generally, this situation is tolerable when $\Gamma_{tot} \simeq$ the resolution, but intolerable when $\Gamma_{tot} \ll$ resolution. To standardize the inclusive measurements of Γ_{tot} the resolution was referenced to the FWHM of the $\psi' \to \gamma\chi_1$ line with the assumption $\Gamma_{tot}(\chi_1) = 0$. For the remaining photon energies the relative resolution was scaled by $1/(E^{1/4}(\mathrm{GeV}))$.

The situation for the exclusive cascade decays is different. The substantially lower photon statistics leads to a less sensitive measure of the FWHM (relative error $\simeq\pm3\%$), while an independent evaluation of the pulls in the kinematic fitting of the events leads to a fixed value for the resolution (no error given).

The best value for $\Gamma_{tot}(\chi_0)$ is (16±4) MeV from the inclusive study, where the error encompasses the uncertainty in resolution. For $\Gamma_{tot}(\chi_2)$ the best value is obtained by averaging the two measurements. The upper limit for $\Gamma_{tot}(\chi_1)$ from the exclusive study, is comparable with an upper limit estimate from the inclusive study based on a quadratic subtraction of the full resolution error.

Following the data in Table III are several comparisons with theory. The absolute estimates are consistently low for $\Gamma_{tot}(\chi_0)$, although the corrections included in the DISP+SR calculation over the lowest order QCD estimates are in the right direction. It would be interesting to see if the spin and relativistic corrections to the wave function, which made such an improvement in the ψ', χ_J dipole matrix elements, could also produce better agreement for the χ_J state full widths. The latter are proportional to the derivative of the wave function at the origin squared. We know of no such predictions. Absolute estimates for $\Gamma_{tot}(\chi_{1,2})$ as well as the ratio of widths are all in agreement with the data, within the very large uncertainties.

TABLE III. χ_J widths and E1 transitions.

DATUM	χ_0		χ_1		χ_2
Observed Mass (MeV)[a]	3416		3510		3556
Resolution FWHM (MeV)					
Inclusive Photons[b]	23.8		17.4		13.9
Exclusive Photons[c]	22.9		16.8		13.4
$\Gamma_{tot}(\chi_J)$ (MeV)					
Inclusive	16 ± 4		Assumed 0		2 ± 1
Exclusive	none		<2.6 (90% C.L.)		4 ± 2
Best Values	16 ± 4		<2.6		3 ± 2
$\Gamma_{tot}(\chi_1)$ Estimate from Experiment + E1 Theory			0.75 ± 0.30		
Theory[d]					
NONREL L+C[14]	2		0.1		0.5
Lowest Order QCD[29]	~2.4		~0.14		~0.64
DISP + SR[31]	4.5 ± .5		--		1.9 ± .3
Relative Widths $\Gamma_{tot}(\chi_J)$					
Crystal Ball	5.3 ± 3.8	:	<2.6	:	1
Lowest Order QCD[29]	3.75	:	0.25	:	1
QCD RADCOR	6.8 ± .4	:	0.17 ± .03	:	1
$BR(\psi' \to \gamma\chi_J \to \gamma\gamma\psi)$[10] (%)	0.059 ± .015		2.38 ± .12		1.26 ± .08
$\Gamma(\chi_J \to \gamma\psi)$ (KeV)					
Crystal Ball	97 ± 38		<700		490 ± 330
NONREL L+C[15]	141		289		398
NONREL QCD	182		381		496
NONREL IS	151		316		422
NONREL CC	130		257		350
NONREL SR	>90 , <180		>200 , <370		>300 , <490
SALPETER	120		258		367
BF L+C	111		244		310
BAG	162		328		415
KG	130		260		340
REL E1	115		215		267
DISP + SR[33]	170 ± 60		245 ± 85		208 ± 72
Relative Rates[e]					
Observed K_γ (MeV)[a]	307		392		432
Crystal Ball	1.0 ± .4	:	<3.5	:	1.8 ± 1.2
Naive E1 Theory	1	:	1	:	1
SALPETER	1	:	1.03	:	1.10
BF L+C	1	:	1.06	:	1.00
KG	1	:	0.96	:	0.94
REL E1	1	:	0.90	:	0.83
QCD E1	1	:	0.80	:	0.81
REL SR	1	:	0.89	:	1.10

a See note *b* in Table II.
b Resolution obtained from $\psi' \to \gamma\chi_1 \to \gamma$ + any, assuming $\Gamma_{tot}(\chi_1) = 0$.
c Resolution obtained from $\psi' \to \gamma\chi_J \to \gamma\psi \to \gamma\ell^+\ell^-$ exclusive channel kinematic fits.
d Neglecting radiative widths.
e Normalized by $1/K_\gamma^3$.

4.3. $\Gamma(\chi_J \to \gamma J/\psi)$

The experimental rate $\Gamma(\chi_J \to \gamma J/\psi)$ may be calculated as follows:

$$\Gamma(\chi_J \to \gamma J/\psi) = \frac{BR(\psi' \to \gamma\chi_J \to \gamma\gamma J/\psi)}{BR(\psi' \to \gamma\chi_J)} \Gamma_{tot}(\chi_J) \quad , \qquad (3)$$

where the product branching ratio in the numerator is obtained from the Crystal Ball exclusive cascade study, the branching ratio in the denominator is from the inclusive photon measurement, and the χ_J full width is as described above. The last three sections in Table III summarize the experimental values and theoretical estimates for the χ_J state radiative widths.

We see from Eq. (3) that the quality of the measurements for $\Gamma(\chi_J \to \gamma J/\psi)$ are dominated by the large uncertainty in $\Gamma_{tot}(\chi_J)$. Consequently, the best measured radiative width is for χ_0. All the models, whether corrected or not, are in agreement with our rates for $\chi_{1,2} \to \gamma J/\psi$. For $\Gamma(\chi_0 \to \gamma J/\psi)$ the spin and relativistic corrected models give slightly better (lower) estimates, in a manner similar to that observed for the E1 transitions from ψ'. The predicted ratio of radiative widths is consistent with our result, which is again dominated by the large error in $\Gamma_{tot}(\chi_J)$. Currently there is an effort underway to measure $\Gamma_{tot}(\chi_J)$ in a resolution independent way using the exclusive cascade decay data, $\psi' \to \gamma_1\chi_J \to \gamma_1\gamma_2 J/\psi$.[36] From the known masses of the ψ' and J/ψ and the two γ energies, two masses are calculated for $M(\chi_J)$, one for each photon, M_1 and M_2. The correlation between M_1 and M_2 will contain a contribution from the states natural line width, which may be extracted by doing a minimum likelihood fit to the correlation probability as a function of Γ_{tot}.

An estimate for the total width of the χ_1 based on i) scaling E1 theory, ii) the measured total width of the χ_0, and iii) Eq. (3) solved for $\Gamma_{tot}(\chi_1)$ is now possible. From i) $\Gamma(\chi_1 \to \gamma_1 J/\psi) = \Gamma(\chi_0 \to \gamma_0 J/\psi)(K_{\gamma_1}/K_{\gamma_0})^3 = (200 \pm 80)$ KeV. Using the measured values for $BR(\psi' \to \gamma\chi_1)$ from Table II and $BR(\psi' \to \gamma\chi_1 \to \gamma\gamma J/\psi)$ from Table III gives $\Gamma_{tot}(\chi_1$ estimate$) = (0.75 \pm 0.30)$ MeV.

4.4. η_c and η_c'

Table IV summarizes the Crystal Ball inclusive photon measurements for the charmonium pseudoscalar candidate particles, and predictions from various models. Regarding the hyperfine splitting (HFS), two of the estimates are based on QCD calculations, REL QCD and DISP+SR, and are in fairly good agreement with our values. A recent determination of the gluonic radiative correction to the HFS, QCD RADCOR, indicates suppression of the splittings which leads to much lower values than observed. In general, the remaining highly model dependent predictions are all in the ball park.

TABLE IV. Charmonium pseudoscalars.

DATUM	η_c	η_c' CANDIDATE
Observed Mass (MeV)[a]	2984 ± 5	3592 ± 5
Hyperfine Splitting (MeV)		
Crystal Ball	111 ± 5	92 ± 5
NONREL QCD	99	65
PERT	75	47
SALPETER	50–95	14–60
BAG	117 (input)	93
REL QCD	115	83
DISP+SR[32]	95 ± 20	--
QCD RADCOR	53 ± 13	23 ± 6
$BR(\psi' \to \gamma\, ^1S_0)$[34] (%)	"Hindered"	"Allowed"
Crystal Ball	$0.29 \pm .08$	0.2–1.3 (95% C.L.)
NONREL L+C[15]	$0.45 \pm .09$	$0.45 \pm .11$
DISP+SR[32]	0.35	--
DISP+SR[33]	<3.7	$.18 \pm .02$
$BR(J/\psi \to \gamma\, ^1S_0)$[34] (%)	"Allowed"	
Crystal Ball	$1.20^{+0.53}_{-0.35}$	N.A.
NONREL L+C[15]	2.6 ± 0.5	
DISP+SR[32]	3.5 ± 0.8	
DISP+SR[33]	2.4 ± 0.9	
$\Gamma_{tot}(^1S_0)$ (MeV)		
Crystal Ball	12.4 ± 4.6	<8 (95% C.L.)
Theory[c]		
QCD gluon counting prediction[b]	4.7 ± 0.9	2–5
DISP+SR[31]	5.6 ± 0.5	--
DISP+SR[32]	4.2 ± 1.0	--
QCD RADCOR	$8.3^{+0.5}_{-0.3}$	$6.9^{+0.5}_{-0.3}$

a See Note *b* in Table II.
b $\Gamma(n^1S_0 \to gg) = \Gamma(n^3S_1 \to ggg)(1/\alpha_s)[27\pi/5(\pi^2-9)]$, $\alpha_s = 0.2$, $\Gamma(1^3S_1 \to ggg) = 48 \pm 9$ KeV, $\Gamma(2^3S_1 \to ggg) = 40 \pm 10$ KeV.
c Neglecting radiative widths.

A precise branching ratio determination for the "allowed" M1 decay, $\psi' \to \gamma\eta_c'$, is hampered by the correlation between the natural width and signal strength for the inclusive photon. Naive M1 theory (NONREL L+C) gives a value within measured limits, and a dispersion theory sum rule calculation, DISP+SR, predicts the branching ratio at our lower limit. Predicted and observed values for the "hindered" M1 transition $BR(\psi' \to \gamma\eta_c)$ are consistent within errors. Here as with the radiative transitions to χ_J, the size of the overlap matrix element is highly dependent on the wave function shapes. These in turn are model dependent and subject to relativistic and spin corrections. The dispersion theory calculation which should be free of these problems is in good agreement. For the M1 "allowed" transition $J/\psi \to \gamma\eta_c$ our measurement is more precise, and the naive M1 theory estimate and dispersion calculations are ~2 times larger thean observed. This is interesting, since the magnetic dipole matrix element is ~1, making the predictions almost model independent. The last section in Table IV covers the η_c and η_c' total widths. The upper limit on the η_c' width is consistent with the naive gluon counting prediction. We measure $\Gamma_{tot}(\eta_c) = (12.4 \pm 4.6)$ MeV, which is good to ±7% error in the inclusive photon energy resolution, and is significantly larger than lowest order QCD estimates. This is very similar to the situation with $\Gamma_{tot}(\chi_0)$. Incorporating gluonic radiative corrections, QCD RADCOR, gives a predicted width within errors of our value.

5. CONCLUSION

Comparing our precise measurements for the E1 transitions $\psi' \to \gamma\chi_J$ with theory has underscored the importance of including i) spin and relativistic corrections, ii) variations in the 2P and 1S wave function shapes resulting from corrections, and iii) coupling to closed and open decay channels. Considering our best measured total widths, i.e., $\Gamma_{tot}(\eta_c)$ and $\Gamma_{tot}(\chi_0)$, it appears that higher order QCD corrections are important and large. Our measurements for the E1 rates $\chi_J \to \gamma J/\psi$ suffer from the large errors in $\Gamma_{tot}(\chi_J)$; our best value is for $\Gamma(\chi_0 \to \gamma J/\psi)$, and the agreement here is slightly better with the corrected theories. Both the potential models and the lowest order QCD derived predictions are capable of consistency with our observed HFS, although QCD radiative corrections appear to go in the wrong direction (less splitting than measured). For the best measured M1 "allowed" pseudoscalar transition, $J/\psi \to \gamma\eta_c$, the naive potential model and dispersion theory predictions are roughly a factor of 2 large. Perhaps corrections to the M1 formula are important.

REFERENCES

1. The Crystal Ball Collaboration: C. Edwards, R. Partridge, C. Peck, F. C. Porter (Caltech); D. Antreasyan, Y. F. Gu, J. Irion, W. Kollman, M. Richardson, K. Strauch, K. Wacker (Harvard); A. Weinstein, D. Aschman, T. Burnett, M. Cavalli-Sforza, D. Coyne, M. Joy, C. Newman, H. Sadrozinski (Princeton); D. Gelphman, R. Hofstadter, R. Horisberger, I. Kirkbride, H. Kolanoski, K. Königsmann, R. Lee, A. Liberman, J. O'Reilly, A. Osterheld, B. Pollock, J. Tompkins (Stanford); E. Bloom, F. Bulos, R. Chestnut, J. Gaiser, G. Godfrey, C. Kiesling, J. Leffler, S. Lindgren, W. Lockman, S. Lowe, M. Oreglia, D. Scharre (SLAC).
2. R. Partridge et al., Phys. Rev. Lett. 45, 1150 (1980).
3. T. M. Himel et al., Phys. Rev. Lett. 45, 1146 (1980).
4. C. Edwards et al., Phys. Rev. Lett. 48, 70 (1982).
5. Cf. Frank C. Porter, "The Hunt for the 1^1P_1 Bound State of Charmonium," these proceedings.
6. J. W. Simpson et al., Phys. Rev. Lett. 35, 699 (1975).
7. J. S. Whitaker et al., Phys. Rev. Lett. 37, 1596 (1976).

8. C. J. Biddick et al., Phys. Rev. Lett. 38, 1324 (1977).

9. J. C. Tompkins, "Recent Results from the Crystal Ball," SLAC Report 224, 578 (1980); E. D. Bloom, in Proceedings of the 1979 International Symposium on Lepton and Photon Interactions at High Energies, ed. by T. Kirk and H. Abarbanel (1979), p. 92.

10. M. Oreglia, Ph.D. thesis, Stanford University, SLAC-236 (1980).

11. Frank C. Porter, CALT-68-853 or SLAC-PUB-2796, September 1981, to appear in Proceedings of the 1981 SLAC Summer Institute on Particle Physics, Stanford, California, ed. by A. Mosher (1981).

12. R. L. Ford and W. R. Nelson, SLAC-210 (1978).

13. G. Karl, S. Meshkov and J. L. Rosner, Phys. Rev. D 13, 1203 (1976).

14. T. Appelquist, R. M. Barnett and K. Lane, Ann. Rev. Nucl. Part. Sci. 28, 387 (1978).

15. E. Eichten et al., Phys. Rev. D 21, 203 (1980).

16. T. Sterling, Nucl. Phys. B141, 272 (1978).

17. W. Buchmüller and S.-H. H. Tye, Phys. Rev. D 24, 132 (1981).

18. C. Quigg and J. L. Rosner, Phys. Rev. D 23, 2625 (1981).

19. A. Martin, Ref.TH.3162-CERN, September 1981, presented at the 1981 EPS International Conference on High Energy Physics, Lisbon, Portugal, July 9-15, 1981.

20. D. Beavis et al., Phys. Rev. D 20, 743 (1979); also see Refs. 14 and 15.

21. M. Krammer and H. Krasemann, Schladming School 1979:259, Lectures given at 18th International Universitatswochen fur Kernphysik, Schladming, Austria, February 28-March 10, 1979; J. D. Jackson, Phys. Lett. 87B, 106 (1979).

22. R. McClary and N. Byers, UCLA/81/TEP/21, contributed to the 1981 International Symposium on Lepton and Photon Interactions at High Energies, Bonn, August 24-29, 1981.

23. J. Baacke et al., DO-TH 81/10, July 1981.

24. E. Eichten and F. Feinberg, Phys. Rev. D 23, 2724 (1981).

25. H. Krasemann, Phys. Lett. 101B, 259 (1981).

26. K. J. Sebastian, PRINT-79-0636, July 1979; K. J. Sebastian, Phys. Lett. 80A, 109 (1980).

27. H. Goldberg, Phys. Rev. D 16, 2243 (1977).

28. A. B. Henriques et al., Phys. Lett. 64B, 85 (1976).

29. R. Barbieri, R. Gatto and E. Remiddi, Phys. Lett. 61B, 465 (1976); R. Barbieri, M. Caffo, R. Gatto and E. Remiddi, Phys. Lett. 95B, 93 (1980); R. Barbieri, R. Gatto and E. Remiddi, Ref.TH.3144-CERN, August 1981.

30. J. Arafune, M. Fukugita, Phys. Lett. 102B, 437 (1981).

31. V. A. Novikov et al., Phys. Lett. 67B, 409 (1977); V. Novikov et al., Phys. Rep. 41C, 1 (1978); M. Shifman et al., Nucl. Phys. B147, 385,448 (1979).

32. M. A. Shifman, JETP Lett. 30, No. 8, 513 (1979); M. A. Shifman, Z. Phys. C4, 345 (1980); M. A. Shifman and M. I. Vysotsky, Z. Phys. C10, 131 (1980).

33. A. Yu. Khodjamirian, EFI-427-34-80 (1980).

34. In comparing branching ratios with theoretical rates, we have used the following experimental values: $\Gamma_{tot}(\psi') = (215 \pm 40)$ KeV and $\Gamma_{tot}(J/\psi) = (63 \pm 9)$ KeV.

35. D. G. Coyne et al., Nucl. Phys. B32, 333 (1971).

36. C. Edwards and R. Partridge, private communication.